Rev. Roum. Sci. Techn.– Électrotechn. et Énerg.
Vol. **62**, *3*, pp. 269–275, Bucarest, 2017

INCREMENTAL CONDUCTANCE BASED MAXIMUM POWER POINT TRACKING CONTROLLER USING DIFFERENT BUCK-BOOST CONVERTER FOR SOLAR PHOTOVOLTAIC SYSTEM

PARTHA SAROTHI SIKDER, NITAI PAL

Key words: Photovoltaic energy conversion, Buck-boost dc-dc converters, Incremental conductance (IC), Maximum power point tracking (MPPT).

Day to day increasing energy demand, depletion of conventional energy sources and harmful effect of global warming open a vent to search alternative energy sources like solar, wind, biomass etc. Now a day, solar energy is one of the prime renewable energy sources because of availability around the globe. The nonlinear *I–V* characteristic of a solar photovoltaic (SPV) cell reduces the efficiency of the overall SPV system during variable solar irradiance and continuous changing temperature. Hence, to maximize the efficiency of the overall SPV system an efficient power conversion technique is compulsory. To maximize the overall efficiency, a dc–dc converter is normally used which is controlled by a maximum power point tracking (MPPT) controller. Here a comparative analysis between different buck-boost converter (conventional buck-boost converter, Cúk, Zeta, and Sepic) is presented for solar photovoltaic application. All the analysis is done in Matlab /Simulink environment and compares the results at the constant temperature condition at variable irradiance and different load are presented here.

1. INTRODUCTION

The conventional sources of electrical energy are insufficient to fulfill the increasing energy demand. In this situation, the renewable energy sources (such as solar, wind biomass etc.) are the only alternative to overcome the energy crisis [1, 2]. Besides them during operation the conventional energy sources which emit harmful greenhouse gases and pollute the environment, but the renewable energy sources do not pollute our environment. Among the renewable energy sources, solar energy grabs the importance because of availability, less maintenance and noiseless operation [3]. The solar photovoltaic cell shows a nonlinear *I–V* (current *vs.* voltage) and *P–V* (power *vs* voltage) characteristic. Hence, to maximize the efficiency a dc-dc converter is very much necessary with a suitable control system to obtain the maximum power at a different solar irradiance, as well as temperature and under variable load.

Instead of conventional boost converter a various buck-boost converter is introduced here to observe the superiority of MPPT technology. To obtain the comparative analysis, a mathematical model of SPV system has been simulated using Matlab/Simulink and compares the obtained result by different dc–dc buck-boost converter. To find out the suitable converter the simulated model has been tested using variable solar irradiance and different load condition. So far, different maximum power point (MPP) finding algorithms are there, among them incremental conductance (IC) algorithm is used here to control the dc–dc converter for simplicity, faster response and easy implementation.

2. BLOCK DIAGRAM OF THE PROPOSED SYSTEM

Figure 1 shows the overall configuration of the solar photovoltaic system.

The system contains an SPV panel which converts solar energy into electricity. The MPPT controllers sense the voltage and current of the SPV panel and deliver a signal to the pulse width modulation (PWM) unit.

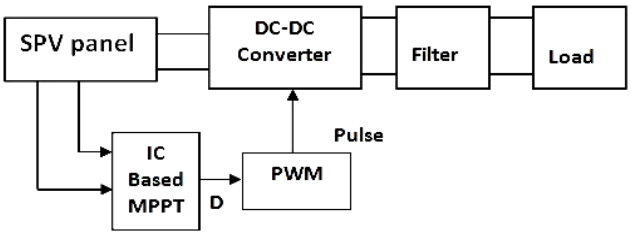

Fig. 1 – Block diagram of proposed system.

The PWM unit delivers a signal to the dc-dc converter which maximizes the power level during variation of solar irradiance as well as variable temperature and load. The filter unit smoothed the output voltage and current profile.

2.1. SOLAR PHOTOVOLTAIC SYSTEMS

The solar energy is converted into electrical energy using solar photovoltaic cells. To obtain a large amount of electrical energy series-parallel connection of multiple solar cells is required, which is termed as an SPV array. Figure 2 shows the equivalent circuit diagram of SPV cell, which consists of photon generated current, a diode, a parallel resistor preventing the leakage current, and a series resistor [2–7].

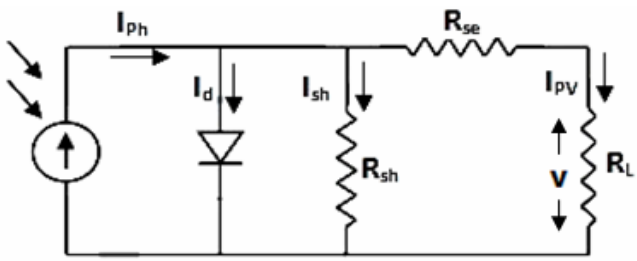

Fig. 2 – Equivalent circuit of SPV cell with load.

Using Kirchhoff's current law the current through the solar cel I_{PV} is obtained as

$$I_{PV} = I_{Ph} - I_d - I_{Sh}. \quad (1)$$

Indian Institute of Technology (Indian School of Mines), Department of Electrical Engineering, Dhanbad – 826004, India, E-mail: parthasarothi.sikder@gmail.com; nitai_pal@rediffmail.com

Here, I_{Ph} is the photocurrent, I_d represents the voltage-dependent current lost to recombination and I_{Sh} represents the shunt resistance current.

$$I_d = I_S\left[e^{\left\{\frac{q\times(V+I_{PV}\times R_{se})}{A\times K\times T}\right\}}-1\right], \quad (2)$$

where I_S represents dark saturation current (at reference temperature, 25^0C), q represents the charge of electron, V represents the output voltage at the load, R_{se} represent the overall voltage drop of the SPV cell, A is the ideality factor, Boltzmann's constant represents by K, T represents the cell temperature (in Kelvin).

The shunt resistance current defines as

$$I_{sh} = \left[\frac{V+(I_{PV}\times R_{se})}{R_{sh}}\right], \quad (3)$$

where R_{sh} represents the shunt leakage resistance of the solar cell.

The light generated current mainly depends both on irradiance and temperature [8–10]. Applying the reference condition the equation the equation modified to

$$I_{Ph} = \left\{I_{SC} + K_i\times(T-T_{ref})\times\frac{\lambda}{\lambda_{ref}}\right\}, \quad (4)$$

where I_{SC} is the short circuit current (at reference temperature, 250°C), K_i represents the short circuit current temperature coefficient at I_{SC}, λ is the solar irradiation [kW/m^2].

If N_S is the numbers of cell connected in series and N_P are the numbers of cell connected in parallel, then the current through the solar array becomes

$$I_{PV} = N_P\times I_{Ph} - N_P\times I_S\left[e^{\left\{\frac{\frac{V}{N_S}+\frac{I_{PV}\times R_S}{N_S}}{V_t}\right\}}-1\right] - \left(\frac{V\times N_P}{N_S}+\frac{I_{PV}\times R_S}{R_{Sh}}\right). \quad (5)$$

Using the above equations a module of sunmodule plus SW 240 poly [11] solar panel is fabricated using MATLAB simulation software and obtains the *P–V* and *I–V* characteristic at different irradiance and temperature which are shown in Figs. 3–6.

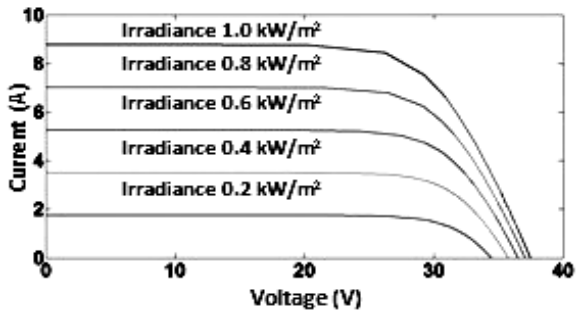

Fig. 3 – *I–V* characteristic of SPV module at different irradiance.

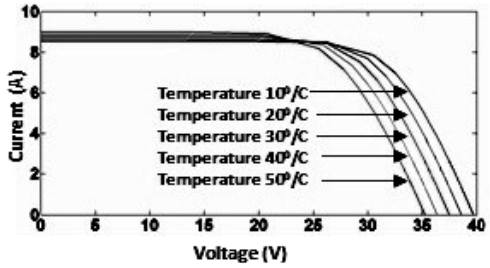

Fig. 4 – *I–V* characteristic of SPV module at different temperature.

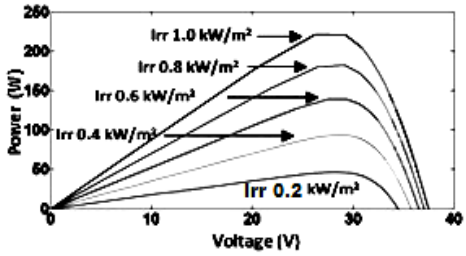

Fig. 5 – *P–V* characteristic of SPV module at different irradiance.

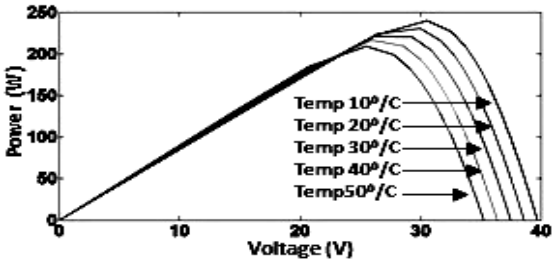

Fig. 6 – *P–V* characteristic of SPV module at different temperature.

3. DC-DC CONVERTER

A dc-dc converter makes the desired changes to obtain a variable dc from a fixed dc. A buck-boost converter is utilized here to maximize the power utilization by a varying duty cycle of the converter at different load and under variable irradiance as well as temperature. The different dc-dc buck-boost converters are shown in Fig. 7 to Fig. 18 [12, 13].

The characteristic of different Buck-Boost converters depends on the mode of the switches. At ON condition, the passive elements stored the energy from the source and supplied to the load during an OFF condition. To obtain the output voltage profile at the load, a volt-second balance equation has been solved at the inductor for different buck-boost converters [12].

3.1. CONVENTIONAL BUCK-BOOST CONVERTER

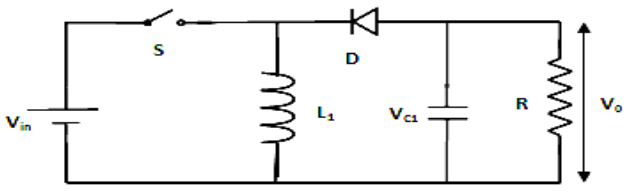

Fig. 7 – Conventional buck-boost dc-dc converter with source and load.

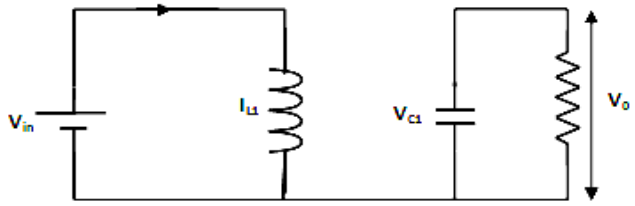

Fig. 8 – Equivalent circuit of buck-boost dc-dc converter at switch ON condition.

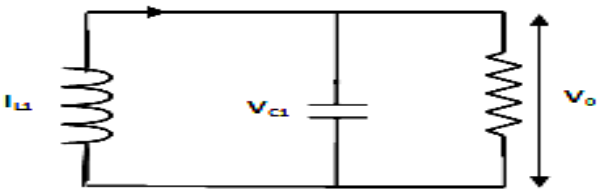

Fig. 9 – Equivalent circuit buck-boost dc-dcconverter at switch OFF condition.

Here only one inductor is present where the volt-second balance at inductor follows

$$V_{in}D - V_0(1-D) = 0$$

$$V_0 = V_{in}\frac{D}{(1-D)} \tag{6}$$

V_0 is the output voltage of the normal buck-boost converter.

3.2. SEPIC BUCK-BOOST CONVERTER

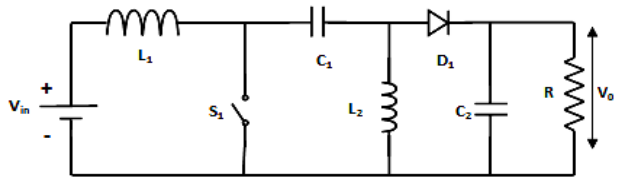

Fig. 10 – Sepic dc-dc converter with source and load.

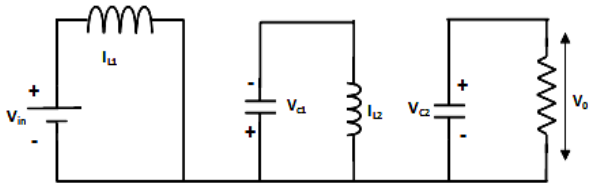

Fig. 11 – Equivalent circuit of Sepic converter at switch ON condition.

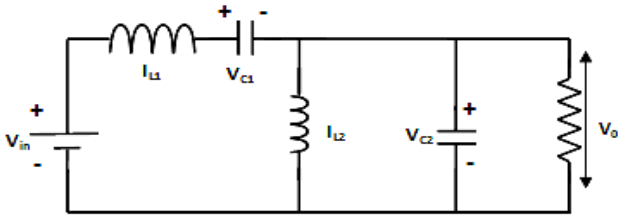

Fig. 12 – Equivalent circuit of Sepic converter at switch OFF condition.

Two inductors are connected in the circuit where the volt-second balance at inductor L_1

$$V_{in}D - (V_{C1} - V_{in} + V_0)(1-D) = 0$$

$$V_{C1} = \frac{V_{in}}{(1-D)} - V_0; \tag{7.1}$$

volt-second balance at inductor L_2

$$V_{C1}D - V_0(1-D) = 0$$

$$V_{C1} = V_0\frac{(1-D)}{D}. \tag{7.2}$$

Now replacing the V_{C1} using equation (7) the output voltage of the Sepic converter

$$V_0 = V_{in}\frac{D}{(1-D)}. \tag{8}$$

where V_0 is the output voltage of the Sepic buck-boost converter.

3.3. CÚK BUCK-BOOST CONVERTER

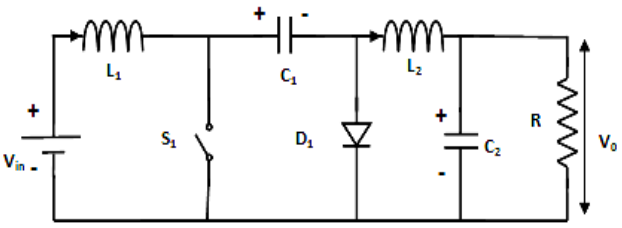

Fig. 13 – Cúk dc-dc converter with source and load.

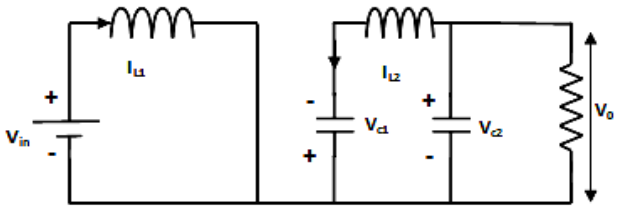

Fig. 14 – Equivalent circuit of Cúk converter at switch ON condition.

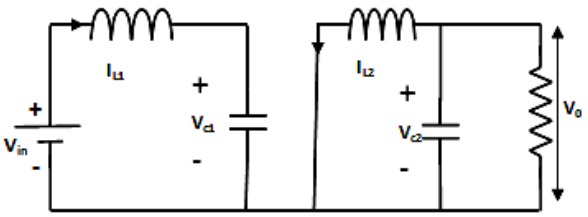

Fig. 15 – Equivalent circuit of Cúk converter at switch OFF condition.

Volt-second balance at inductor L_1

$$V_{in}D - (V_{in} - V_{C1})(1-D) = 0$$

$$V_{C1} = \left(\frac{V_{in}}{1-D}\right). \tag{9.1}$$

volt-second balance at inductor L_2

$$(V_0+V_{C1})D + V_0(1-D) = 0$$

$$V_0 = -DV_{C1}. \tag{9.2}$$

Now replacing the V_{C1} using equation (9) the output voltage of the Cúk converter is

$$V_0 = -\frac{DV_{in}}{(1-D)}. \tag{10}$$

where, V_0 is the output voltage of the Cúk buck-boost converter.

3.4. ZETA BUCK-BOOST CONVERTER

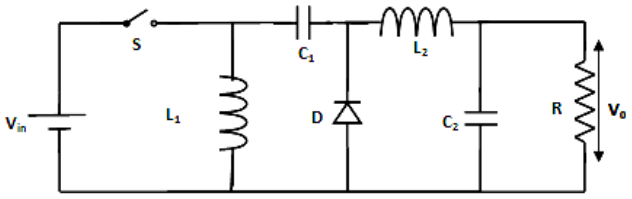

Fig. 16 – Zeta dc-dc converter with source and load.

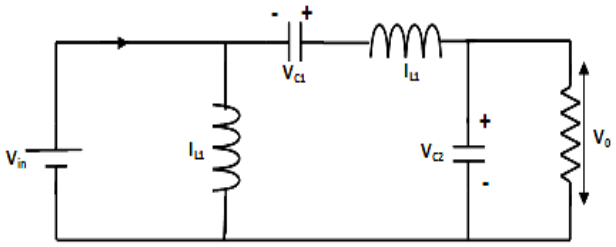

Fig. 17 – Equivalent circuit of Zeta converter at switch ON condition.

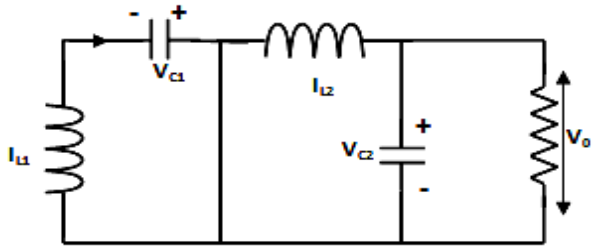

Fig.18 – Equivalent circuit of Zeta converter at switch OFF condition.

Volt-second balance at inductor L_1

$$(V_{in}+V_{C1}-V_0)D - V_0(1-D) = 0 \tag{11.1}$$

$$V_{C1} = \left(\frac{V_0}{D}\right) - V_{in}.$$

volt-second balance at inductor L_2

$$V_{in}D - V_{C1}(1-D) = 0 \tag{11.2}$$

It results

$$V_0 = V_{in}\frac{D}{(1-D)}. \tag{12}$$

where V_0 is the output voltage of the Zeta buck-boost converter.

4. IC BASED MPPT CONTROLLER

The incremental conductance method of MPPT controller senses the power output (voltage and current) of a PV array and finds the maximum power condition. Mathematically the output power sensed by the PV module P is derived as follows [13–17].

$$\frac{dP}{dV} = \frac{d(VI)}{dV} = I + V\frac{dI}{dV} = 0. \tag{13}$$

For the validity of the MPP condition the above equation is reduced to

$$\frac{I}{V} = -\frac{dI}{dV}. \tag{14}$$

The equation (13) shows that the network conductance increases when the operating zone is on the left hand side of the PV curve and the network conductance decreases when the operating zone is on the right hand side which is shown in Fig. 19.

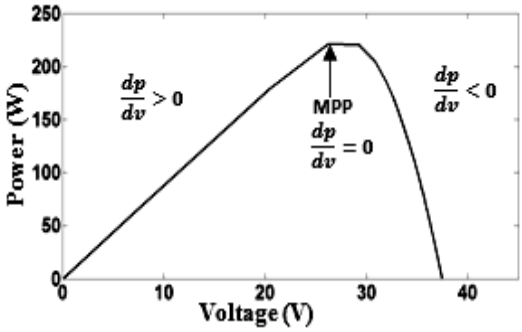

Fig. 19 – Operating power P and voltage V curve of the conventional IC algorithm.

The counter senses the present power $P(k) = V(k{\cdot}I(k)$ and compared to the present power with the previous power $P(k-1) = V(k-1){\cdot}I(k-1))$ and changes the duty cycle to reach the MPP within a few moments which is shown in equation (15)

$$\frac{dI}{dV} = -\frac{I}{V};\ \left(\frac{dP}{dV} = 0\right). \tag{15}$$

Left hand side of the MPP denoted as

$$\frac{dI}{dV} > -\frac{I}{V};\ \left(\frac{dP}{dV} > 0\right). \tag{16}$$

Right hand side of the MPP denoted as

$$\frac{dI}{dV} < -\frac{I}{V};\ \left(\frac{dP}{dV} < 0\right). \tag{17}$$

The algorithm related to IC based MPPT controller is shown in Fig. 20, where k represents the counter and D represents the duty cycle. During operation the duty cycle, which is fed to the dc-dc converter, is simultaneously changed to obtain the MPP condition at different irradiance as well as temperature.

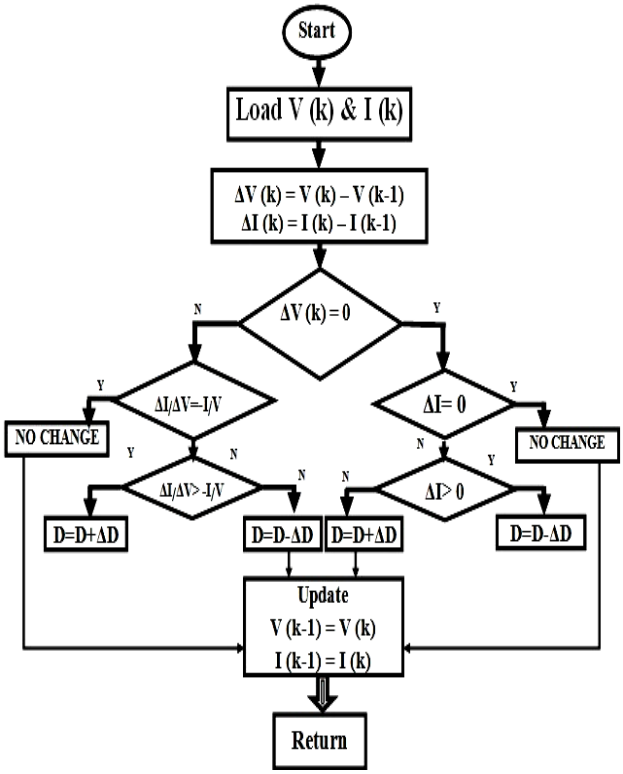

Fig. 20 –Flow chart of incremental conductance algorithm

5. RESULTS AND DISCUSSION

To obtain a comparative result among different buck-boost converters, the passive elements of the converter made similar except for the filter capacitor of conventional buck-boost converter to reduce the oscillation which is shown in Table 1. At the same operating frequency, the output power of the different converter then compared to find out the suitable buck-boost converter for MPPT controller.

Table 1

Sl. No.	Converter	L_1 [mH]	L_2 [mH]	C_1 [μF]	C_2 [μF]
1	Sepic	0.1	50	10	1500
2	Cúk	0.1	50	10	1500
3	Zeta	0.1	50	10	1500
4	Buck-Boost	0.1	-----	1500	----

For simplicity the variable irradiance is considered only and makes the temperature constant at 30^0 C. The irradiance of the suns varies with respect to time T seconds and observer the controller performance within the same time period .The variable solar irradiance which is considered here is shown in Fig. 21.

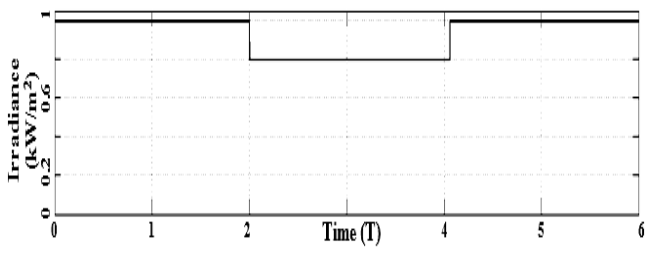

Fig. 21 – Variable irradiance taken for the analysis.

Figure 22 shows the output power of different buck-boost dc-dc converters (conventional buck-boost, Sepic, Cúk, and Zeta) as well as without an MPPT connected system. Considering 1 Ω resistive load the MPPT connected system abstracts almost double power compared to directly connected system. The conventional buck-boost converter is the fastest than the other but the power output is more fluctuating compared to the other buck-boost converter.

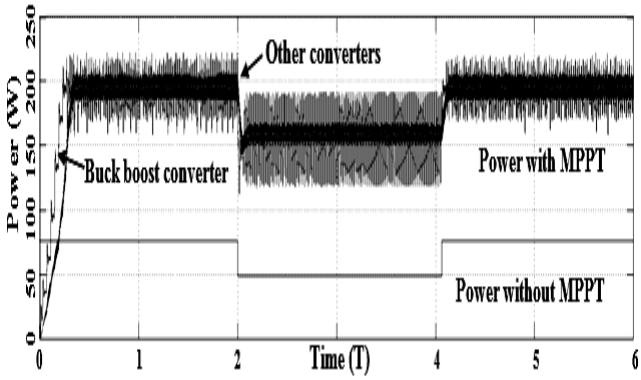

Fig. 22 – Output power for different buck-boost converter and without converter topology for 1 Ω resistive load.

Figure 23 shows the power output of MPPT controller connected different buck-boost converters. The controller tracks MPP point within 0.4 second initially and letter it tracks the change of irradiance within 0.1 second. The buck-boost converter is the fastest among the other converters initially. But the output power characteristic of the Cúk and Zeta converter is better than the conventional buck-boost and the Sepic converter. The output power oscillation is very low in case of Cúk and Zeta converter compared to the other converters.

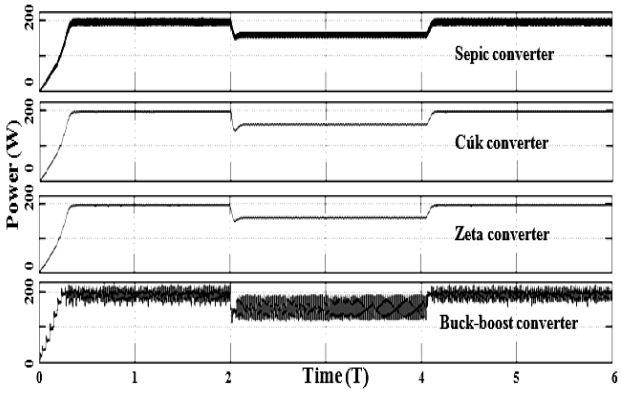

Fig. 23 – Output power for different buck-boost converter only for 1 Ω resistive load.

For 10 Ω load also the MPPT connected SPV system provides more power compared to direct connected without an MPPT connected system which is shown in Fig. 24. The conventional buck-boost converter also abstracts more power than a direct connected system, but less than Sepic, Cúk, and Zeta converter.

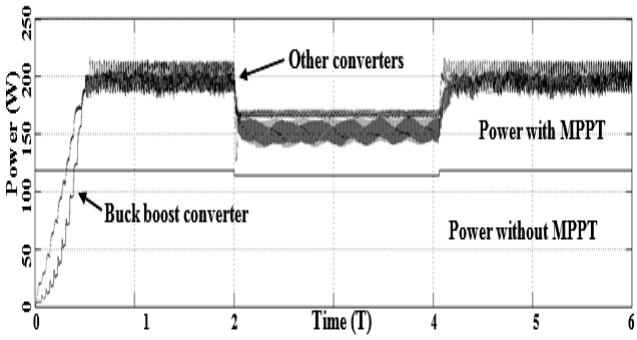

Fig. 24 – Output power for different buck-boost converter and without converter topology for 10 Ω resistive load

For 10 Ω resistive load all the converters provide oscillation. Only the Cúk and Zeta converters output power is less oscillatory this is shown in Fig. 25.

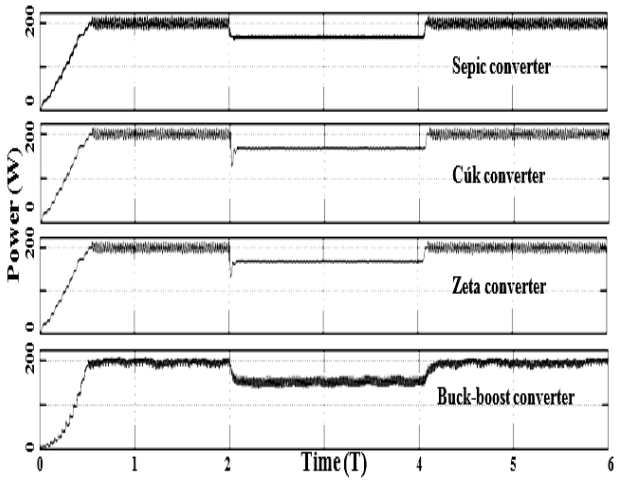

Fig. 25 – Output power for different buck-boost converter only for 10 Ω resistive load.

Figure 26 shows the comparative result of buck-boost, Sepic, Cúk, and Zeta converter output power. The Sepic, Cúk, Zeta converter, abstract more than double power compared to direct connected SPV system. The conventional buck-boost converter output power is slightly less than the other converters and tracking speed is also less than the Sepic, Cúk, and Zeta converter.

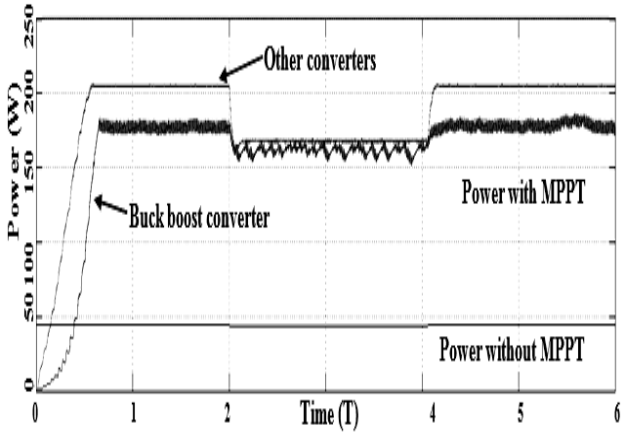

Fig. 26 – Output power for different buck-boost converter and without converter topology for 30 Ω resistive load.

Figure 27 shows the comparative result of output power of conventional buck-boost, Sepic, Cúk, Zeta converters. Here the Sepic converter output power oscillation reduces but the output power oscillation of Cúk and Zeta is similar and less oscillatory compared to Sepic converter. Only conventional buck-boost converter produces less power, low tracking speed and large oscillation during operation.

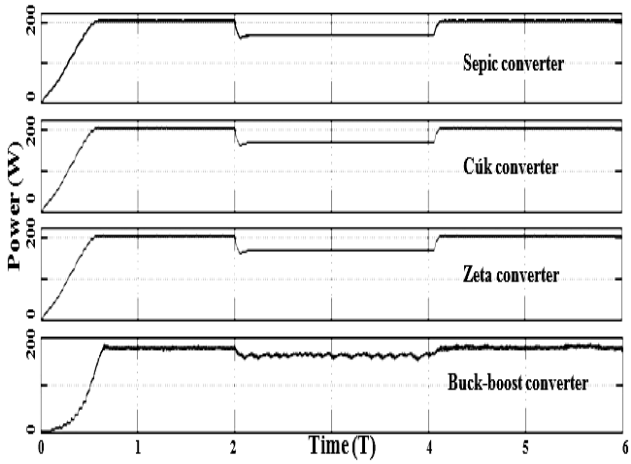

Fig. 27 – Output power for different buck-boost converter only for 30 Ω resistive load.

6. CONCLUSIONS

In this study a 240 W solar module and IC based MPPT controller is simulated using Matlab/Simulink and test the performance of MPPT controller using different buck-boost converters. To study the comparative result variable solar irradiance considered here and 1 Ω, 10 Ω and 30 Ω resistances are considered as a load. Due to MPPT controller for different load as well as different irradiance the all the buck-boost converters extract more energy compared to a directly connected SPV system. Among the four buck-boost converter the output power for Sepic, Cúk and Zeta extract more power and with less oscillation than conventional buck-boost converter. Among the three (Sepic, Cúk and Zeta), Cúk and Zeta converter power output is similar and less oscillatory compared to Sepic converter. Hence under variable solar irradiance and different load condition the Cúk and Zeta converter connected IC based MPPT controller performance is better compared to Sepic and conventional buck-boost converter.

ACKNOWLEDGEMENTS

The authors are grateful for the Indian Institute of Technology (Indian School of Mines), Dhanbad and University Grants Commission, Bahadurshah Zafar Marg, New Delhi, India for granting financial support under the major research project entitled “Development of Hybrid Off-grid Power Supply System for Remote Areas [UGC Project: F. No. 42-152/2013(SR), w.e.f. 01/04/2013]” and are also grateful to the Under Secretary and Joint Secretary of UGC, India for their active cooperation.

Received on December 17, 2016

REFERENCES

1. Ioan Felea, Vasile Moldovan, Daniel Albuț, *Specificities in analysis of energy availability Generated by photovoltaic sources*, Rev. Roum. Sci. Techn. – Électrotechn. et Énerg., **61**, *1*, pp. 42–47 (2016).
2. Ahmed Jubaer, Salam Zainal, *A Modified P&O Maximum Power Point Tracking Method with Reduced Steady-State Oscillation and Improved Tracking Efficiency*, IEEE Transactions on Sustainable Energy, **7**, *4*, pp. 1506–151 (2016).
3. Salim Bouchakour, Ahmed Tahour, Houari Sayah,Kamel Abdeladim, Aissaoui Abdelghani, *Direct Power Control of Grid Connected Photovoltaic System with Linear Reoriented Coordinate Method as Maximum Power Point Tracking Algorithm*, Rev. Roum. Sci. Techn. – Électrotechn. et Énerg., **59**, *1*, pp. 57–66 (2014).
4. Dorin Petreus, Daniel Moga, Adina Rusu, Toma Patarau, Mihai Munteanu, *Photovoltaic System with Smart tracking of the Optimal Working Point*, Advances in Electrical and Computer Engineering, **10**, 3, pp. 40–47 (2010).
5. Karel Zaplatilek, Jan Leuchter, *Behavioral Model of Photovoltaic Panel in Simulink®*, Advances in Electrical and Computer Engineering, **11**, *4*, pp. 83–88 (2011).
6. Spasoje Mirić, Miloš Nedeljković, *The solar photovoltaic panel simulator*, Rev. Roum. Sci. Techn. – Électrotechn. et Énerg., **60**, *3*, pp. 273–281 (2015).
7. Hocine Abdelhak Azzeddine, Mustapha Tioursi, Djamel-Eddine Chaouch, Brahim Khiari, *An offline trained artificial neural network to predict a photovoltaic panel maximum power point*, Rev. Roum. Sci. Techn. – Électrotechn. et Énerg., **61**, *3*, pp. 255–257 (2016).
8. M.G. Villalva , J.R. Gazoli , E.R. Filho, *Comprehensive approach to modeling and simulation of photovoltaic arrays*, IEEE transactions on power electronics, **24,** *5*, pp. 1198–1208 (2009).
9. M. Louzazni , E.H. Aroudam , H.Yatimi, *Modeling and Simulation of A Solar Power Source for a Clean Energy without Pollution*, International Journal of Electrical and Computer Engineering (IJECE), **3**, *4*, pp. 568–576 (2013).
10. R. Schoenmake, *Developing a smart grid simulation model from an end-users perspective*, Master Thesis, University of Groningen Faculty of Mathematics and Science, Groningen, 2014.
11. Solar World Sunmodule™, *Solar Panel 240 Watt Data Sheet*, https://www.solarworld-usa.com Date of search on 10.10.2016
12. Nedmohan, Torem. Undeland, William P. Robbins, *Power Electronics Converters, Applications, and Design*, John Wiley & Sons, Inc., New York – London – Sydney, 2011, pp. 163–194.
13. Muhammad H. Rashid, *Power Electronics Handbook Devices, Circuits, and Applications*, Elsevier Inc. All rights reserved, USA, 2011, pp. 414–542.
14. Ali Durusu, Ismail Nakir, Ali Ajder, Ramazan Ayaz, Hakan Akca, Mugdesem Tanrioven, *Performance Comparison of Widely-Used Maximum Power Point Tracker Algorithms under Real Environmental Conditions*, Advances in Electrical and Computer Engineering, **14**, *3*, pp. 89–94 (2014).
15. Mehmet Ali Ozcelik, Ahmet Serdar Yilmaz, *modification of the incremental conductance algorithm in grid connected photovoltaic systems*, Rev. Roum. Sci. Techn.– Électrotechn. et Énerg. **61**, *2*, pp. 164–168, (2016).
16. M.T. Makhloufi., Y. Abdessemed, M.S. Khireddine, *An Efficient ANN-Based MPPT Optimal Controller of a DC/DC Boost Converter for Photovoltaic Systems*, Automatika, pp. 109–119 (2016).
17. Amine Attou, Ahmed Massoum, Mohammed Chadli, *Comparison of two tracking methods for photovoltaic system*, Rev. Roum. Sci. Techn. – Électrotechn. et Énerg, **60**, *2*, pp. 205–214 (2015).